Hot spot stress and fatigue performance of bird-beak SHS X-joint under brace in-plane bending

Bin Cheng[1*], Fenghua Huang[1], Chen Li[1], Xiaoling Zhao[2]

[1]*Department of Civil Engineering, Shanghai Jiao Tong University, Shanghai 200240, China*

[2]*Department of Civil and Environmental Engineering, UNSW, Sydney, NSW 2052, Australia*

**cheng_bin@sjtu.edu.cn*

Bird-beak X-joints are a new type of square hollow section (SHS) welded joints and their fatigue performances are of great attentions due to the stress concentrations. Therefore, the stress concentrations and fatigue performances of such innovative joints under brace in-plane bending were investigated. The static loading was first conducted to obtain the stress concentration factors (SCFs). Refined finite element models were established to reveal the influences of the non-dimension parameters β, 2γ and τ on the SCFs. Cyclic loading was sequentially employed, and the fatigue behaviors including failure mode, fatigue life and rigidity degradation, were all observed. The results show that for both square and diamond joints, the global maximal SCFs always occurred at brace crown spots Cr-F or Cr-A, and the diamond bird-beak joints provided lower SCFs than square ones with identical dimensions. Furthermore, the comparison with the IIW code *S-N* design curves also indicates that the *S-N* design curves proposed for convention ones could be also useful to estimate the fatigue life of bird-beak joints under brace in-plane bending.

Keywords: Square hollow section, bird-beak X-joints, hot spot stress, fatigue performance, in-plane bending.

1 Introduction

The bird-beak SHS joints, including square and diamond type, were generated by rotating the one member or both two members of conventional X-joints at 45° about their longitudinal axes, resulting in an aesthetical appearance. It has been proved by Ono et al. (1991), Owen et al. (1996) and Chen et al. (2015) that the structural rigidities and static strengths of bird-beak joints both behave better than those of conventional ones.

While for the structures under repeated load, the fatigue behaviors of the connections are much more significant than the static behaviors. However, few researches focused on this filed. Ishida (1992) first conducted the fatigue test on the bird-beak T-joints considering the load case of cyclic brace axial force. Keizer et al. (2003) investigated the stress concentration factors of diamond bird-beak joints under brace axial force. In recent years, extensive studies were carried out to improve the applications of such innovative joints. Tong et al. (2015, 2016) investigated the hot spot stresses and fatigue behaviors of diamond bird-beak T-joints under axial force and in-plane bending. Cheng et al. (2014, 2015, 2018) mainly focused on the stress concentrations of bird-beak joints under several loading cases, where fatigue behaviors were also observed.

Therefore, this research focused on the stress concentrations and fatigue performances of bird-beak joints under brace in-plane bending. Static loading was first conducted to achieve the

Proceedings of the 17th International Symposium on Tubular Structures.
Editors: X.D. Qian and Y.S. Choo

Published by Research Publishing, Singapore.
ISBN: 978-981-11-0745-0; doi:10.3850/978-981-11-0745-0_106-cd

hot spot stress and SCFs, and the influences of three non-dimensional parameters (i.e., β, γ and τ) were also investigated on SCFs. Fatigue test was sequentially employed, and the fatigue behaviors including failure mode and fatigue life, as well as the rigidity degradation, were all observed.

2 Specimens and test setup

2.1 Dimensions and hot spots

Bird-beak SHS X-joints, including square and diamond types, were employed to study the stress concentrations and fatigue performances under brace in-plane bending. The X-joints were designed by considering three non-dimensional parameters, that are, brace/chord width ratio $\beta=b_1/b_0$, chord wall slenderness ratio $2\gamma=b_0/t_0$, and brace/chord wall thickness ratio $\tau=t_1/t_0$, where L_0 and L_1 represent the length of the chord and the brace, respectively, b_0 and t_0 represent the sectional width and wall thickness of the chord, respectively, and b_1 and t_1 represent the sectional width and wall thickness of the brace, respectively. The dimension details of the specimens are listed in Table 1.

Referring to the achievements of Cheng et al (2014), four crown hot lines (Cr-B and Cr-C in the chord, Cr-A and Cr-F in the brace) and six saddle hot lines (Sa-B, Sa-C and Sa-D in the chord, Sa-A, Sa-E and Sa-F in the brace) were selected for hot spot stress measurements (see Fig. 1).

Table 1. Non-dimensional parameters of bird-beak X-joints

Specimen	Non-dimensional parameters		
	β	2γ	τ
S-IPB-X1	0.45	17.39	0.661
S-IPB-X2	0.60	21.05	0.474
D-IPB-X1	0.45	17.39	0.661
D-IPB-X2	0.60	21.05	0.474

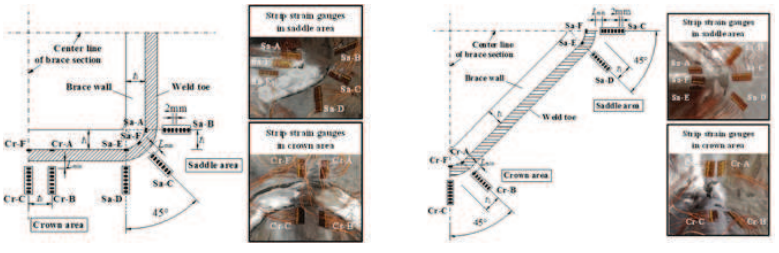

(a) Square (b) Diamond

Fig 1. Arrangement of strip gauges at hot spots

2.2 Test rig and procedure

Fig. 2 shows the typical test rig for static loading and fatigue loading, respectively, where the

chord's upper end was connected to the actuator via spherical hinge, and the chord's lower end was free, besides, the two brace ends was simply supported. A concentrated force was applied on the chord upper end so that a pair of reaction forces were subsequently generated at the brace ends, which making the specimens under brace in-plane bending. The static loading was conducted prior to the fatigue loading to obtain the SCFs and hot spot stress, from which a reasonable load amplitude for fatigue test was achieved. To record the accurate time of the crack initiation, several high detection (HD) cameras were arranged to focus on the potential cracking locations. Besides that, the barometers were connected to the chord and brace ends to monitor the air pressure variations in the tubes, so that the occurrence of the through-thickness cracks could be recorded.

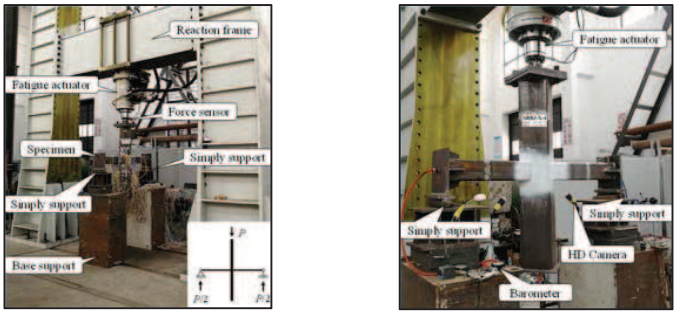

(a) Static loading (b) Fatigue loading

Fig. 2. Test rig

3 Discussion on experimental SCFs

The experimental SCFs at selected hot spots was summarized in Table 2, where both left and right sides are considered. All SCFs were calculated as $SCF=c\cdot(\Delta\varepsilon_h/\Delta\varepsilon_{nom\,s})$, where $\Delta\varepsilon_{hs}$ and $\Delta\varepsilon_{nom}$ are the extrapolated hot spot strain and measured nominal strain, respectively, and c is the factor describing the relationship between SCF and strain concentration factor (SNCF) (Cheng, 2018). Herein, the factor c takes the value of 1.10, 1.15 respectively for brace and chord spots of square joints, while of 1.10, 1.20 respectively for brace and chord spots of diamond joints.

For the square bird-beak joints, the SCFs in the crown area are obviously higher than those in the saddle area. The greatest crown SCFs, which occurred at spot Cr-F, were found to be only 41%~45% of the greatest saddle SCFs which occurred at spot Sa-B. Moreover, the most serious stress concentrations occurred at spot Cr-F or Cr-A, with the SCFs being high as 2.61~4.10. While for the diamond bird-beak joints, the saddle area hardly generated stress concentrations since the saddle area is located at the natural axis, resulting in the stress along the hot lines being closed to zero. The brace SCFs at spot Cr-A and Cr-F are higher than the chord SCFs at spot Cr-B and Cr-C, and the greatest brace SCFs, which occurred at the hot spot Cr-F, were 43%~46% higher than the greatest chord SCFs which occurred at spot Cr-C. Comparatively, the square bird-beak joints perform higher SCFs than diamond ones with same dimensions.

Table 2. Experimental SCFs

Specimen	Location	SCF for chord spots					SCF for brace spots				
		Cr-C	Cr-B	Sa-D	Sa-C	Sa-B	Cr-F	Cr-A	Sa-E	Sa-F	Sa-A
S-IPB-X1	Left side	1.18	1.20	0.93	1.09	1.13	2.77	2.61	1.03	1.02	0.99
	Right side	1.16	1.13	1.00	1.09	1.12	2.78	2.70	1.10	1.05	0.94
S-IPB-X2	Left side	1.23	1.18	1.39	1.58	N/A	4.10	4.08	1.43	N/A	N/A
	Right side	N/A	1.13	1.39	1.47	1.81	3.98	3.69	1.47	1.31	1.34
D-IPB-X1	Left side	1.08	0.75	0.13	0.02	0.14	1.90	1.66	0.17	0.06	0.17
	Right side	1.07	0.75	0.14	0.02	0.14	1.96	1.65	0.15	0.04	0.18
D-IPB-X2	Left side	1.08	0.89	0.18	0.03	N/A	2.02	1.89	0.09	0.07	0.09
	Right side	1.10	0.86	0.17	N/A	0.14	2.04	1.89	0.12	N/A	0.08

4 Numerical simulation on SCFs

4.1 Finite element models and validation

A refined finite element (FE) model of bird-beak X-joints was established by ANSYS to further reveal the influences of the three non-dimensional parameters on SCFs. The fillet welds were accurately simulated due to their significant effects on the stress concentrations. The solid element SOLID95 with 20 nodes and three degrees of freedom for each node was adopted. Considering the complexities of stress distributions near the weld junction, the meshes within these areas were refined. The element sizes within the extrapolation regions were taken as 2 mm, and the meshes within transition regions were taken as 4 mm. Fig. 3 illustrates the comparisons of numerical and experimental SNCFs, it is found that the numerical results are consistent well with the test results. Therefore, the finite element model established herein is considered as accurate enough for the following investigation.

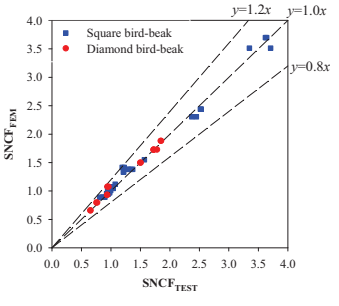

Fig 3. Comparison of numerical SNCFs with experimental SNCFs

4.2 Parametric study

(1) Square bird-beak joints

Fig. 4 illustrates the SCF variations against the three non-dimensional parameters (i.e., β, γ

and τ) for square bird-beak joints, where crown hot spots Cr-C, Cr-F and saddle hot spots Sa-D, Sa-E were typically selected. As can be found, the SCFs at the four selected hot spots first increase and then decrease as β varies from 0.3 to 1.1, and the β corresponding to the curve peak ranges between 0.8 and 1.1. This variation can be explained by the geometry induced stiffness discontinuity which considered as the nature cause of the stress concentration. As β increases, the brace walls move from the chord's lateral corner area to the chord's middle corner, as a result the stiffness differences between the brace walls and chord walls first be enlarged and then decrease, which causes the parabolic variations of SCFs. In case of 2γ, the SCFs almost increase linearly as 2γ varies from 12.5 to 25. For the 2γ, the SCFs will become enlarged or slightly decrease as τ varies from 0.25 to 1.0. This also can be explained by the stiffness differences between chord and brace wall at junction area.

(2) Diamond bird-beak joints

Fig. 5 illustrates the SCFs variations at specified hot spots against the β, 2γ and τ for diamond bird-beak joints. In case of β. As β varies from 0.3 to 0.7, the crown SCFs at spots Cr-C and Cr-F become enlarged almost linearly. This trend can be explained by the stiffness differences between brace walls and chord walls, which is similar with the square joints. In case of 2γ, the SCFs at crown area are enlarged as 2γ varies from 12.5 to 25.0. In case of τ, the parabolic variations of SCFs at crown area are very evident, and the increasing rates of SCF variations decrease as the τ becomes enlarged. While the influence on the saddle SCF variations is meaningless since the SCFs are very close to zero at saddle area.

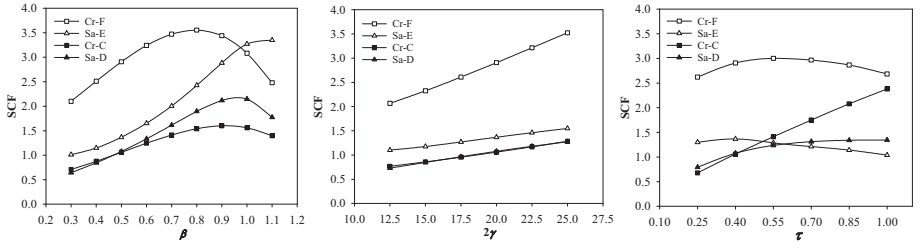

(a) Against β (2γ=20, τ=0.4) (b) Against 2γ (β=0.5, τ=0.4) (c) Against τ (β=0.5, 2γ=20)

Fig. 4. SCF variations of square bird-beak joints

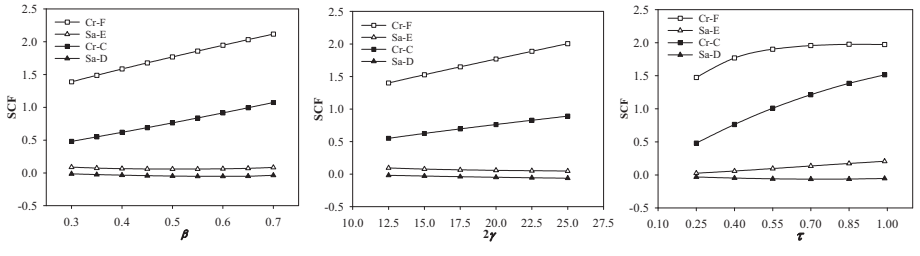

(a) Against β (2γ=20, τ=0.4) (b) Against 2γ (β=0.5, τ=0.4) (c) Against τ (β=0.5, 2γ=20)

Fig 5. SCF variations of diamond bird-beak joints

5 Discussion on fatigue behaviors

5.1 Fatigue mode

Fig. 6 shows the typical failure modes of the square and diamond bird-beak X-joints under fatigue loading. It can be found that the fatigue cracks are observed only on the tension side of brace surfaces for both two types of bird-beak joints.

For the square type, the cracking process can be divided into three stages, that are, Stage I: The crack initiated at the weld toe near the spots Cr-A and Cr-F, where the SCF is proved to be maximum. After initiation, the crack extended its two tips both exactly along the weld toe. Stage II: As cyclic load continued, two tips of the crack grew away from the weld toe and propagated obliquely on the brace wall. Stage III: The crack further propagated on the brace surface, and bypassed the brace corner to extend its two tips on the lateral sides of the brace. The fatigue failure occurred due to the accumulative long crack reaching the ultimate length.

While for the diamond type, the cracking process can be divided into two stages, that are, Stage I: Similar with the square bird-beak joint, the crack was initiated at the weld toe at the brace crown area. Stage II: As cyclic load continued, the crack further extended exactly along the welded toe until touched the brace saddle area. Finally, the fatigue failure occurred due to the crack length reaching the ultimate value.

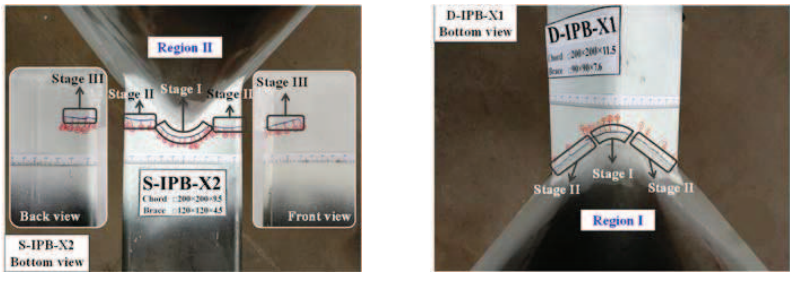

(a) Square joint (b) Diamond joint

Fig 6. Fatigue mode of the bird-beak SHS X-joint

5.2 S_{rhs}-N design curve

Three types of fatigue lives, that are, crack initiation life N_2, through-thickness crack life N_3, fatigue life N_4, were observed during the fatigue test. The obtained fatigue lives were compared with the IIW code (2008) S_{rhs}-N design curves, which was proposed for the conventional SHS joints, as shown in Fig. 7. For the square joints, the N_4 is located on or near the IIW design curve, but the N_2 and N_3 are slightly below the design curves. Regarding, the diamond joints, all fatigue life data are all located on or near the design curve. Therefore, considering the absence of sufficient test data, the IIW code S_{rhs}-N design curves could be also useful to assess the fatigue lives for bird-beak joints under cyclic brace in-plane bending if the hot stress and SCFs are identified. However, the probable cracking during the service life cycle should be paid great attention.

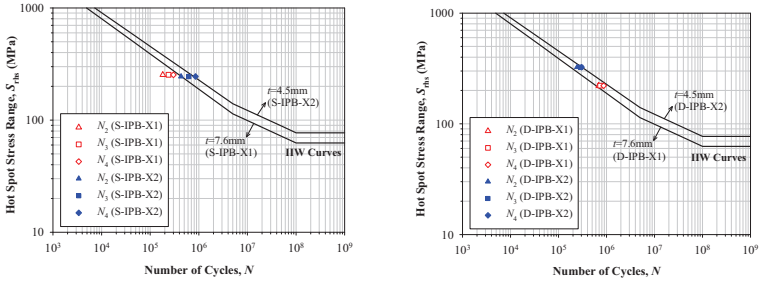

(a) Square joint (b) Diamond joint

Fig 7. Comparison between fatigue lives and IIW design curves

5.3 Rigidity degradation

The variations of vertical displacement range at the brace end against the number of load cycles are illustrated in Fig. 8, where the original vertical displacement f_0 is nominalized against the real-time vertical displacement f, and the number of load cycles N is nominalized against the trough-thickness life N_3. During the early stage (i.e., N<0.8N_3), the vertical rigidity decreased quite slowly and the degradations were totally within 3%. After crack penetrating the wall thickness (i.e., N> N_3), the rates of rigidity degradations were observed to increase sharply, indicating that the occurrence of the through-thickness cracks would induce significant rigidity degradation of the bird-beak joints. Eventually, the rigidity degradations were found about 27%~39% as the cracks reached the ultimate length. Comparatively, the diamond joints were observed to own more remarkable rigidity degradation rates than that of the square joints under fatigue loading.

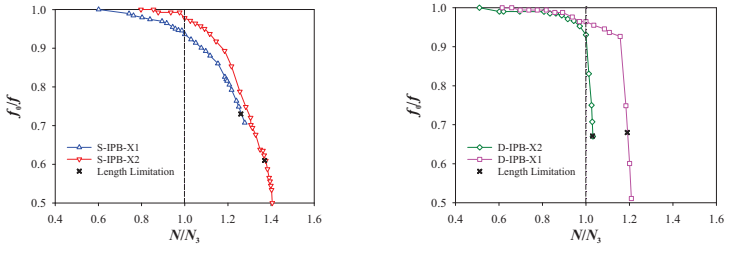

(a) Square joint (b) Diamond joint

Fig 8. Normalized axial displacement at brace end versus normalized number of cycles

6 Conclusions

The stress concentrations and fatigue performances of the bird-beak joints subjected to brace in-plane bending were investigated by using experimental and numerical methods. The results show that the most serious stress concentrations always occurred at spot Cr-F or Cr-A, with the SCFs being high as 2.61~4.10 and 1.65~2.04, respectively for the square and diamond types. Comparatively, the square bird-beak joints provide higher SCFs than diamond ones with identical

non-dimensional parameters. The fatigue crack initiated at the weld toe near the spots Cr-A and Cr-F, where the SCFs are prove to be relatively higher. Furthermore, the IIW code S_{rhs}-N design curves proposed for convention ones could be also used to estimate the fatigue lives of bird-beak joints under brace in-plane bending.

Acknowledgements

The research herein was sponsored by the National Natural Science Foundation of China (no. 51678359) National Key Research and Development Program of China (No. 2016YFB1200602-28, 2016YFB1200601-B27). The supports are gratefully acknowledged.

References

Ono, T. Iwata, M. Ishida, K., An experimental study on joints of new truss system using rectangular hollow sections. *Proceeding of International Symposium on Tubular Structures*, 344-353, London, 1991.

Owen, J.S. Davies, G. Kelly, R.B., A comparison of the behaviour of RHS bird beak T-joints with normal RHS and CHS systems. *Proceeding of International Symposium on Tubular Structures*, 173-180, London, 1996..

Y. Chen, R. Feng, J. Wang. Behaviour of bird-beak square hollow section X-joints under in-plane bending. *Thin-Walled Struct* 86: 94-107, 2015.

Ishida, K., Experimental research on fatigue behavior of diamond bird-beak joint. *Proc., Symp. on Structural Engineering, Architectural Institute of Japan, Tokyo* (in Japanese), 1992.

Keizer, R. Romeijn, A. & Wardenier, J. Glijnis, P.C., The fatigue behaviour of diamond bird beak T-joints. *10th International Symposium on Tubular Structures (ISTS10)*, 303-310, Spain, 2003.

Tong, L.W. Xu, G.W. Liu Y.Q. Yan, D.Q. Zhao, X.L. Finite element analysis and formulae for stress concentration factors of diamond bird-beak SHS T-joints. *Thin-Walled Struct.* 86: 108-120, 2015.

Tong, L.W. Xu, G.W. Yan, D.Q. Zhao, X.L. Fatigue tests and design of diamond bird-beak SHS T-joints under axial loading in brace. *Journal of Constructional Steel Research* 118: 49-59, 2016.

Cheng, B. Qian, Q. Zhao, J.C. Lu, Z.A. Zhao, X.L. Stress concentration factors of square bird-beak SHS T-joints under brace axial loading. *15th International Symposium on Tubular Structures (ISTS15), Rio de Janeiro*, 343-348, 2015.

Cheng, B. Qian, Q. Zhao, X.L. Tests to Determine stress concentration factors for square Bird-Beak SHS joints under chord and brace axial forces. *ASCE's J. Struct. Eng.* 140(11): 04014088, 2014.

Cheng, B. Qian, Q. Zhao, X.L. Numerical investigation on stress concentration factors of square bird-beak SHS T-joints subject to axial forces. *Thin-walled Struct.* 94: 435-445, 2015.

Li C, Huang FH, Lou Y, Cheng B. Stress concentration factors of bird-beak SHS X-joints under brace axial forces. *J. Constr. Steel Res* 150: 87-98, 2018.

IIW. *Recommended Fatigue Design Procedure for Welded Hollow Section Joints*. In: Zhao XL, Packer JA, editors. Part 1: Recommendations, Part 2: Commentary, XV-1035-99; 2008.